AGU PUBLICATIONS

Geophysical Research Letters

RESEARCH LETTER
10.1002/2015GL066090

Key Points:
- Plasmapause locations under quiet geomagnetic conditions
- Plasmaspheric bulge in the dusk sector
- Quiet time plasmapause extended toward geosynchronous orbit

Correspondence to:
K.-H. Kim,
khan@khu.ac.kr

Citation:
Kwon, H.-J., K.-H. Kim, G. Jee, J.-S. Park, H. Jin, and Y. Nishimura (2015), Plasmapause location under quiet geomagnetic conditions ($Kp \leq 1$): THEMIS observations, *Geophys. Res. Lett.*, *42*, 7303–7310, doi:10.1002/2015GL066090.

Received 5 SEP 2015
Accepted 8 SEP 2015
Accepted article online 12 SEP 2015
Published online 30 SEP 2015

Plasmapause location under quiet geomagnetic conditions ($Kp \leq 1$): THEMIS observations

H.-J. Kwon[1], K.-H. Kim[2,3], G. Jee[1], J.-S. Park[4], H. Jin[2], and Y. Nishimura[5]

[1]Division of Climate Change Research, Korea Polar Research Institute, Incheon, Korea, [2]School of Space Research, Kyung Hee University, Yongin, Korea, [3]Solar-Terrestrial Environment Laboratory, Nagoya University, Nagoya, Japan, [4]Institute of Space Science, National Central University, Jhongli, Taiwan, [5]Department of Atmospheric and Oceanic Science, University of California, Los Angeles, California, USA

Abstract We statistically examined the plasmapause location (L_{pp}) under quiet geomagnetic conditions ($Kp \leq 1$) using the electron density inferred from the Time History of Events and Macroscale Interactions during Substorms (THEMIS) spacecraft potential for 2 year period (2008 and 2009). Five hundred forty-three L_{pp} samples were identified under steady quiet conditions with Kp values ≤ 1 during 12 h prior to the plasmapause crossing. From our large data set, we determined the medians and means of L_{pp} in L and magnetic local time (MLT). They are located near geosynchronous orbit and nearly circular. The L_{pp} medians show a slight bulge located in postdusk sector. Comparing with previous models, our median or mean L_{pp} is extended ~1–2 L from the Earth than the model L_{pp} along the local time from 0800 to 2400 MLT. That is, L_{pp} locations in the previous models are underestimated during quiet geomagnetic conditions.

1. Introduction

The plasmasphere is a region in the inner magnetosphere filled with dense and cold plasma of ionospheric origin. The region typically extends ~4–5 Earth radii (R_E) from the ionosphere along the magnetic equator. The plasmasphere is bounded by a sharp density gradient region, called the plasmapause, in which the density gradient is a factor of 5 or more over an L distance smaller than 0.5 [e.g., *Carpenter and Anderson*, 1992]. Since the radial location of the plasmapause is controlled by a combination of the corotational and solar wind-driven convectional electric fields, the size and shape of the plasmasphere depend on the level of geomagnetic activity. Empirical plasmapause location models [e.g., *Chappell et al.*, 1970; *Carpenter and Anderson*, 1992; *Moldwin et al.*, 2002; *O'Brien and Moldwin*, 2003] show a clear trend of decreasing plasmapause L shell with increasing Kp.

A bulge in the dusk sector is expected from the effect of an interaction between convection and corotation electric fields. This bulge has been observed to rotate toward noon and midnight with increasing and decreasing geomagnetic activity, respectively [*Carpenter*, 1970; *Higel and Wu*, 1984; *Moldwin et al.*, 1994]. During high geomagnetic activity, the bulge is observed at the compressed dayside magnetopause [*Kim et al.*, 2007]. The dynamical evolution of the plasmaspheric bulge has been reported using the IMAGE/EUV data providing global images of the plasmasphere [*Goldstein et al.*, 2004]. However, some observational studies reported that signatures of the bulge are not clearly formed in the dusk sector [e.g., *Moldwin et al.*, 2002].

The location of the plasmapause is overlapped with the region of ring current and radiation belts. Thus, the plasmapause location is one of the important parameters to understand the plasma properties in the inner magnetosphere through particle-particle and wave-particle interactions [e.g., *Gary et al.*, 1994; *Summers et al.*, 2007]. It has been reported that electromagnetic ion cyclotron (EMIC) waves interact with approximately MeV electrons in the region near the plasmapause located at $L = 4–5$ [e.g., *Nishimura et al.*, 2014]. Recently, *Hyun et al.* [2014] suggested that the EMIC waves excited near the plasmapause located near geosynchronous orbit play a significant role for relativistic electron loss into the atmosphere through strong pitch angle scattering under quiet geomagnetic conditions.

In previous empirical plasmapause models using geomagnetic Kp index [e.g., *Moldwin et al.*, 2002; *O'Brien and Moldwin*, 2003], the estimated plasmapause is located within $L = 6$ under quiet geomagnetic conditions ($Kp \leq 1$). It should be noted that the number of plasmapause crossings under quiet geomagnetic conditions

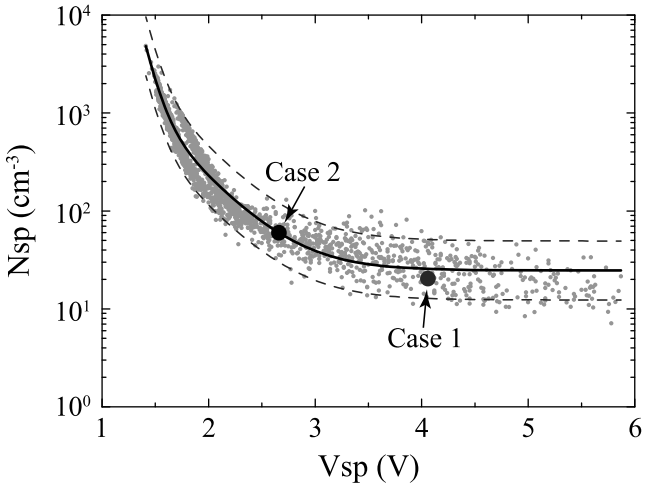

Figure 1. N_{SP} as a function of the spacecraft potential (V_{SP}) for all plasmapause crossing events. The solid line is the best fit deduced from data points, and the two dashed curves indicate factor of 2 margins of error for the best fit. Small dots indicate the individual plasmapause crossings, and two large dots indicate two case events presented in section 3.

in those previous models is very small compared to that under moderate geomagnetic conditions. Thus, the estimated quiet time plasmapause locations may have a large uncertainty.

In our study we statistically examined the plasmapause location under quiet geomagnetic conditions ($Kp \leq 1$) using the electron density inferred from the Time History of Events and Macroscale Interactions during Substorms (THEMIS) spacecraft potential. Two year period (2008 and 2009) was chosen for analysis because both years were marked by extremely weak solar wind conditions. When $Kp \leq 1$, 1103 plasmapause crossings were identified , and 543 crossings out of them were identified under steady quiet conditions with Kp values ≤ 1 during 12 h prior to the plasmapause crossing. From our large data set, median and mean statistics are taken in L and magnetic local time (MLT). We compare the median/mean plasmapause locations obtained in our study and the locations estimated from previous studies [*Gallagher et al.*, 2000; *Moldwin et al.*, 2002; *O'Brien and Moldwin*, 2003].

2. Data Set and Plasmapause Identification

In order to identify the plasmapause location under quiet geomagnetic conditions ($Kp \leq 1$), we use the total electron density (N_{SP}) inferred from the spacecraft potential and electron thermal speed measured by the Electric Field Instrument [*Bonnell et al.*, 2008] and electrostatic analyzer (ESA) instrument [*McFadden et al.*, 2008] on board THEMIS A, D, and E probes [*Angelopoulos*, 2008] in 2008 and 2009, when solar activity is uncommonly weak. A computer code converting the spacecraft potential to the electron density is developed by *Nishimura et al.* [2013] using the method proposed by *Mozer* [1973] and *Pedersen et al.* [1998]. The code has been provided from the THEMIS website (http://themis.ssl.berkeley.edu/software.shtml). N_{SP} has been used to identify the plasmapause [e.g., *Li et al.*, 2010; *Nishimura et al.*, 2013, 2014]. *Takahashi et al.* [2010] validated N_{SP} estimated from the spacecraft potential around the plasmapause using toroidal wave frequencies (see Figure 9 in their study). It has been noted that N_{SP} has an uncertainty within a factor of ~2 [*Pedersen et al.*, 1998]. In order to examine whether the "factor of 2" uncertainty can be applied to the THEMIS data, we plot N_{SP} as a function of the spacecraft potential (V_{SP}) for all plasmapause crossings identified in our study, mentioned later, in Figure 1. The solid line is the best fit deduced from THEMIS data, and the two dashed curves indicate factor of 2 margins of error for the best fit. The individual plasmapause crossings are shown by small dots. The two examples shown in the next section are marked with large dots. For $2 < V_{SP} < 3$, N_{SP} is good to within a factor of 2. For $V_{SP} < 2$ and $V_{SP} > 3$, however, the data points are bounded by the two dashed lines, implying that N_{SP} is within a factor of 4. Since N_{SP} has a factor of ~2–4 uncertainties, we also use the electron density (N_{ESA}) obtained from the electrostatic analyzer (ESA) density moment [*McFadden et al.*, 2008] to identify the plasmapause. Comparing N_{SP} and N_{ESA}, we can determine whether N_{SP} increase is due to the increase of the energetic electron flux or due to the increase of cold electrons (i.e., cold plasmaspheric plasmas) below the energy cutoff (a few eV) of ESA.

The location of the plasmapause is usually identified by a density gradient of a factor of 5 or greater over an L distance smaller than 0.5. This criterion had been used to identify the plasmapause location in previous studies [*Carpenter and Anderson*, 1992; *Moldwin et al.*, 2002]. In this study, we use the same criterion used in previous studies to determine the plasmapause, and the plasmapause is defined as the innermost sharp gradient in density. This inner edge of the steep gradient is denoted as L_{pp}. A computer algorithm identifies a potential L_{pp} for all inbound and outbound THEMIS A, D, and E orbits of the plasmasphere. In order to ensure that L_{pp} is the boundary of the main plasmasphere, the examination of N_{SP} and N_{ESA} data for the inbound and outbound plasmapause crossings was done by visually reading the data. Multiple and structured plasmapause crossings were not used in this study.

During the 2 year period (2008–2009) in our study, the data for 3737 inbound and outbound legs were available. Using the selection procedure, we were able to determine L_{pp} for 2075 (~55 %) out of the 3737 possible plasmapause crossings. In *Moldwin et al.* [2002], an identifiable plasmapause was observed on 73% of the inbound and outbound trajectories. The lower percentage of L_{pp} identification on the inbound and outbound legs in our study may be due to the interval of 2008–2009 in which geomagnetic activity was unusually low. In the very quiet times, the plasma density distribution becomes very gradual in the radial direction [*Carpenter and Anderson*, 1992]. Thus, such gradual plasmapause crossings were not satisfied from our L_{pp} definition.

Under quiet geomagnetic conditions ($Kp \leq 1$), we were able to determine 1103 (~53%) L_{pp} out of 2075 plasmapause crossings. It is found that 534 (~26%) out of 2075 L_{pp} crossings occurred under moderate ($2 \leq Kp < 4$) geomagnetic conditions. In order to compare the estimated L_{pp} from previous empirical models [e.g., *Moldwin et al.*, 2002], we also examined L_{pp} under "steady quiet conditions" with Kp values ≤ 1 during 12 h prior to the plasmapause crossing. Five hundred forty-three (~49%) out of 1103 L_{pp} samples were identified under steady quiet conditions.

3. Observations and Comparison With Previous Models

Figure 2a shows an inbound plasmapause crossing (case 1) by THEMIS D near midnight (MLT = ~23.0) at L = ~6.3 on 19 May 2009. The blue and red lines indicate N_{SP} and N_{ESA}, respectively. THEMIS D was in the plasma sheet from the beginning of the plot (12:00 UT) to ~12:24 UT and then moved across the plasmapause around 12:24 UT, which is clearly identified by a sudden increase in N_{SP} (marked by the vertical dashed line). At that time, Kp was 1−. The maximum Kp in the previous 12 h for this plasmapause was also 1−. Thus, THEMIS D crossed the plasmapause under steady quiet geomagnetic conditions. According to the empirical model by *Moldwin et al.* [2002] using Kp(12max) = 1, where Kp(12max) indicates the maximum Kp observed in the previous 12 h prior to the plasmapause crossing, the plasmapause is located around L = 5.3, which is ~1.0 L more inward than the location of the plasmapause shown in Figure 2. As THEMIS D was crossing the plasmapause and entered the plasmasphere, the significant difference between N_{SP} and N_{ESA} appeared for the interval of ~12:24–13:00 UT. This indicates that the spacecraft encountered cold plasmaspheric plasmas.

Figure 2b shows the energy spectra of electrons measured from ESA on board THEMIS D. The enhanced electron flux in the energy range from 200 eV to 3 keV clearly shows an energy-dependent signature. That is, lower energy electrons are injected more deeply toward the plasmapause than higher-energy electrons. Those electrons are the plasma sheet electrons. Thus, the inner edge of the plasma sheet coincides with the plasmapause location near midnight.

Figure 3 shows a dayside (MLT = 14.1) plasmapause crossing (case 2) at 13:34 UT (marked by the vertical dashed line) on 1 September 2008 by THEMIS A . The L_{pp} was identified at L = 6.75, under quiet geomagnetic condition (Kp = 1−). The maximum of Kp over the 12 h interval prior to the plasmapause crossing was 1+. Therefore, this event was not included for the case under steady quiet conditions. There is an appearance of a significant difference between N_{SP} and N_{ESA} from 13:34 to 14:00 UT. Thus, we suggest that THEMIS A entered the main plasmasphere at 13:34 UT. Similar to the energy flux signatures shown before the plasmapause crossing near midnight shown in Figure 2b, there is a clear energy-dependent signature of electron flux in the energy range of ~200–800 eV before the dayside plasmapause crossing.

Figures 4a–4f show the location of the spacecraft in the L-MLT coordinates for the L_{pp} events under moderate ($2 \leq Kp < 4$), quiet ($Kp \leq 1$), and steady quiet conditions ($Kp \leq 1$ for 12 h before L_{pp} crossing). Figures 4g–4i show the local time distribution of L_{pp} events for each geomagnetic condition. In Figures 4a–4c the individual

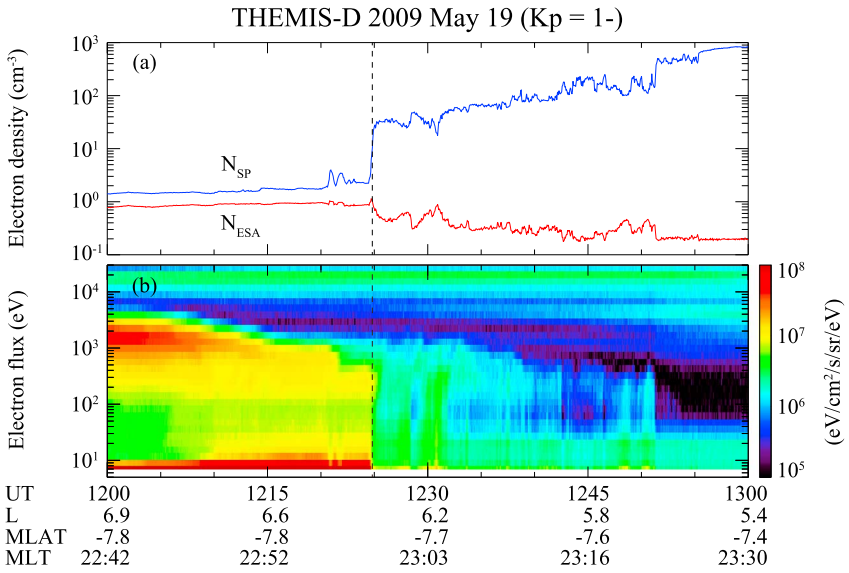

Figure 2. Observations of the plasmapause crossing by THEMIS D on 19 May 2009. (a) Electron density (blue) determined from the spacecraft potential and electron density (red) determined from the ESA particle data. (b) Energy-time spectrogram of electrons. The vertical dashed line indicates the plasmapause crossing.

crossings of L_{pp} are shown by small dots. The large dots connected by a straight line are the medians of L_{pp} events within 1 h MLT bin except for the region of 1800–2400 MLT under steady quiet conditions. Since the number of samples is small in 1800–2400 MLT under steady quiet conditions as shown in Figure 4i, the median statistics are made in 2 h MLT bin on that region. The radial bars connect the lower and upper quartiles for each median, a blue circle indicates geostationary orbit ($L = 6.7$), and four magnetic L shells ($L = 4$, 6, 8, and 10) are drawn with the dashed lines. Figures 4d–4f are plotted the same as Figures 4a–4c but mean L_{pp} values are plotted in a given local time bin. We note that the longitudinal signature of L_{pp} medians for a given geomagnetic condition is very similar to that of L_{pp} means.

Under moderate geomagnetic conditions, most of samples are bounded within $L = 6$ except for the region from 1600 to 2000 MLT in which the data points are scattered considerably. The hourly medians/means for L_{pp} samples show an asymmetry along the local time. The medians/means near midnight are slightly larger than those near noon. This noon-midnight asymmetry was reported by *Moldwin et al.* [2002]. It is clearly shown

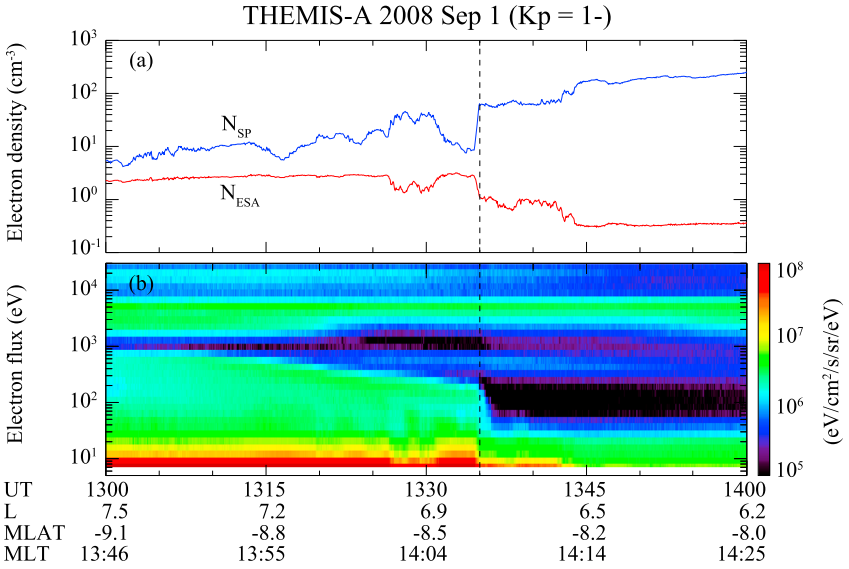

Figure 3. The format is the same as Figure 1 except for THEMIS A on 1 September 2008.

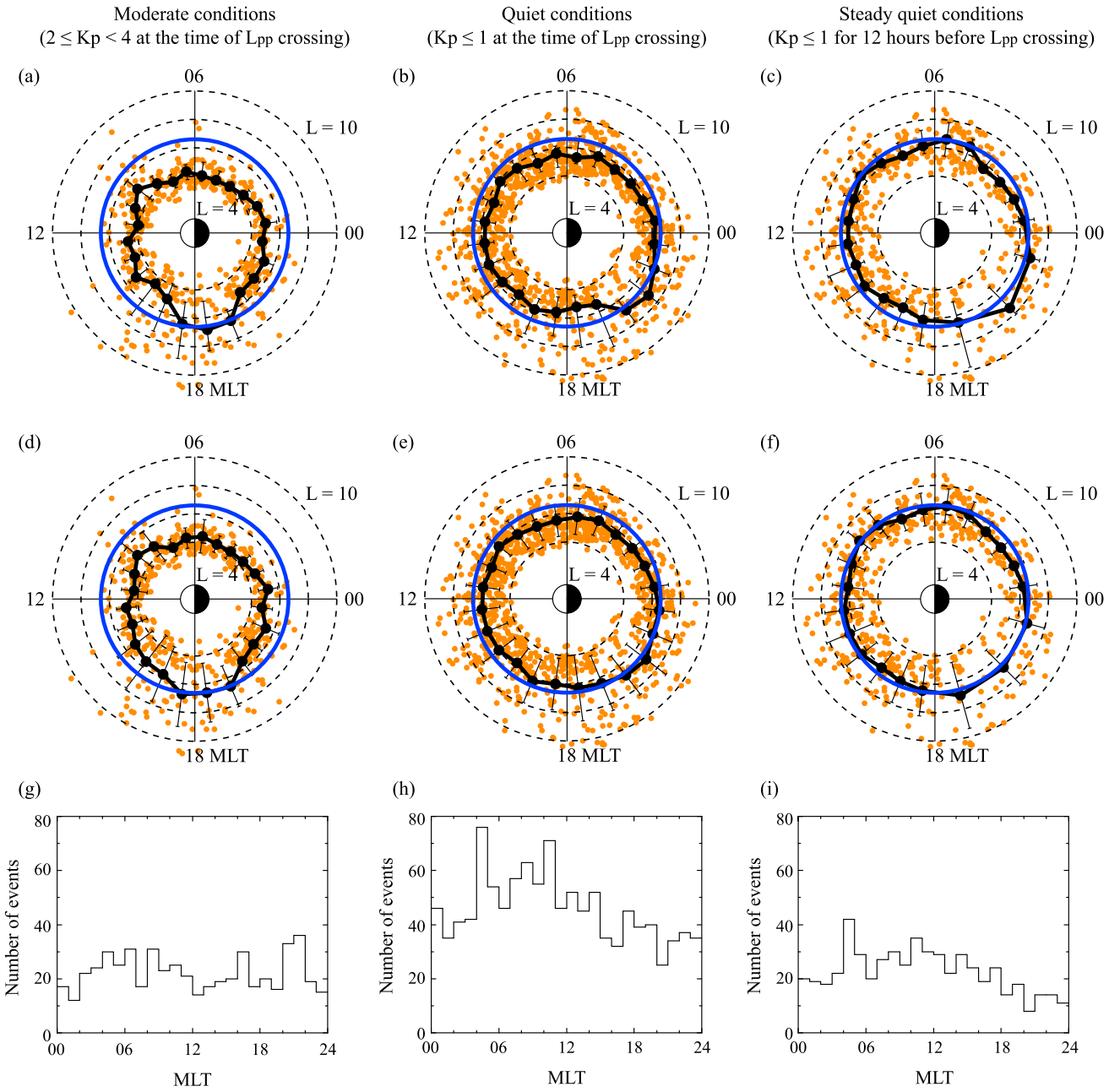

Figure 4. The location of the spacecraft in the *L*-MLT coordinates for the L_{pp} samples under (a and d) moderate ($2 \leq Kp < 4$), (b and e) quiet ($Kp \leq 1$), and (c and f) steady quiet conditions ($Kp \leq 1$ for 12 h before L_{pp} crossing). (g–i) The local time distribution of L_{pp} samples under a given geomagnetic condition. The blue circle indicates geosynchronous orbit. See the text for descriptions.

that there is a plasmapause bulge on the duskside. The median/mean values on the bulge are located near geosynchronous orbit. This longitudinal distribution of the median/mean plasmapause is very similar to that reported by *Chappell et al.* [1971] (see their Figure 1).

The data points for L_{pp} under quiet geomagnetic conditions are mainly distributed in the range between $L = \sim 4$ and $L = \sim 8$. There are many plasmapause crossings found at all local times of geosynchronous orbit. This indicates that the plasmasphere extends to larger *L* values. Although there is a considerable spread of the data, the hourly medians/means for L_{pp} are located near $L = 6$, and their longitudinal structure is nearly circular. The L_{pp} medians show a slight bulge near 2000–2200 MLT sector, for which the medians of L_{pp} are located above geosynchronous orbit. In that local time, the mean L_{pp} values are also slightly larger than the geosynchronous *L* value.

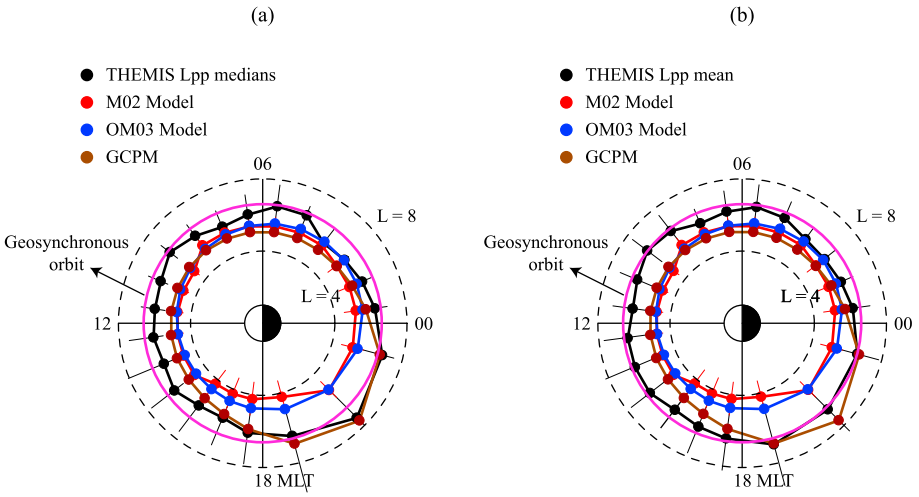

Figure 5. (a) A comparison of L_{pp} median values obtained from THEMIS observations under steady quiet conditions and the estimated L_{pp} from previous models provided by *Gallagher et al.* [2000] (Global Core Plasma Model, GCPM), *Moldwin et al.* [2002] (M02), and *O'Brien and Moldwin* [2003] (OM03) with $Kp = 1$. (b) The format is the same as Figure 5a but for THEMIS L_{pp} mean values.

Figures 4c and 4f show the spatial distributions of L_{pp} for which the *Kp* conditions remained steady (i.e., $Kp \leq 1$) for 12 h prior to the plasmapause crossing. The longitudinal structure of the median/mean L_{pp} under steady quiet conditions is similar to that under quiet condition. At all local times the L_{pp} medians/means under steady quiet conditions are larger than those under quiet conditions and distributed near geosynchronous orbit. The median at 2100 MLT clearly show extended plasmapause radius above geosynchronous orbit. This slight bulge is longitudinally extended from 1900 to 2300 MLT at geosynchronous orbit. The local time width of the bulge and centroid of the bulge are similar to those reported by *Higel and Wu* [1984] under quiet geomagnetic conditions.

4. Discussion

Under moderate geomagnetic conditions, the median values of L_{pp} show the plasmaspheric bulge in the dusk sector. It is well known that the larger L_{pp} near dusk is due to a superposition of a corotational electric field and a solar wind-induced electric field in the dawn-dusk direction in that local time sector. This dawn-dusk L_{pp} asymmetry leads to longitudinally asymmetric nightside plasmapause. That is, the median locations of the plasmapause in postmidnight are closer to the Earth than those in premidnight. It has been known that the frequency of Pi2 pulsation is determined by the size of the plasmasphere and reported that Pi2 frequency decreases as the plasmapause distance increases [*Takahashi et al.*, 2003]. *Kwon et al.* [2012] observed that the average Pi2 frequency spectrum for average *Kp* values of ~2 shows a continuous structure, smoothly increasing from ~10 mHz in the premidnight sector to ~20 mHz in the postmidnight sector (see Figure 16 in their study), and suggested that the local time dependence of Pi2 frequency is due to larger plasmapause distance in premidnight than in postmidnight. Such a nightside asymmetry of the plasmapause distance with respect to the Earth is confirmed in Figures 4a and 4d.

We found the relatively circular distribution of the median and mean L_{pp} located near geosynchronous orbit during quiet geomagnetic conditions. This longitudinal structure is due to the fact that the Earth's corotational electric field dominates plasma flow at near geosynchronous orbit. Thus, the bulge plasma that formed around 1800 MLT under moderate conditions rotates with the main plasmasphere and moves toward later local times with decreasing geomagnetic activity. The appearance of the slight bulge near postdusk (2000–2200 MLT) sector under quiet conditions in Figures 4b and 4c may be explained with this argument.

The main purpose of this study is to compare the estimated L_{pp} from previous models and the L_{pp} values in our study. Figure 5 shows a comparison of L_{pp} median and mean values obtained from THEMIS observations under steady quiet conditions and L_{pp} derived from previous models provided by *Gallagher et al.* [2000] (Global Core Plasma Model, GCPM), *Moldwin et al.* [2002] (M02), and *O'Brien and Moldwin* [2003] (OM03) with $Kp = 1$. The error bars are marked with the radial lines. In previous studies the error bar indicates a degree

of scatter from the slope determined by the linear fit to L_{pp} events selected under all *Kp* conditions. In our study, however, the radial error bars are obtained from the L_{pp} events only under quiet geomagnetic conditions ($Kp \leq 1$). Thus, the meaning of the length of the radial "error" bars in our study is not the same as that in previous studies.

Figure 5a shows that the L_{pp} values derived from GCPM are in good agreement with the L_{pp} medians from 1600 to 0300 MLT. At other local times, however, L_{pp} positions from GCPM are located earthward of the medians about 1 *L*. Since our mean L_{pp} does not show a weak bulge in the postdusk sector as shown in Figure 5b, there is a slight difference between GCPM model and L_{pp} means in that local time region. The L_{pp} locations predicted by M02 and OM03 are similar to those from GCPM for the region between 0300 and 1600 MLT. Therefore, M02 and OM03 models predict L_{pp} values about 1 *L* smaller than our L_{pp} medians and means. Since there is no bulge signature on the dusk-midnight sector in both M02 and OM03 models, the difference of the radial distance between the L_{pp} medians and model L_{pp} values increases as much as ~2 *L* in the 2000–2200 MLT region. Thus, L_{pp} locations in previous models are underestimated during quiet geomagnetic conditions.

We suggest two possible reasons for the difference between our result from THEMIS spacecraft data and M02 study using the CRRES spacecraft data. First, the CRRES spacecraft had an apogee at the geocentric distance of 6.3 R_E with an inclination of 18°. Thus, the spacecraft will miss the plasmapause formed above geosynchronous orbit (i.e., $L > 7$). This is why M02 has a upper limit of $L = 7$ for the distribution of L_{pp} events during quiet geomagnetic conditions (see Figure 4 in M02). Second, small number (about 20) of L_{pp} events distributed in a large range between $L = 2$ and $L = 7$ during quiet condition ($Kp \leq 1$) were used for linear fitting in M02. This indicates that "steady quiet geomagnetic condition" (i.e., the maximum *Kp* in the previous 12 h ≤ 1) did not occur frequently while the CRRES spacecraft was operated in 1990–1991 (solar maximum). As mentioned above, however, our samples are taken from the solar minimum year 2008–2009. This solar minimum was marked by periods of very weak solar wind conditions contributing to quiet geomagnetic conditions [e.g., *Kwon et al.*, 2013]. We identified 543 L_{pp} events, which is a factor of ~25 more L_{pp} events than M02, under steady quiet geomagnetic conditions. Thus, we suggest that our median and mean L_{pp} statistics made in *L* and MLT are not unreasonable.

Acknowledgments
The THEMIS data were obtained from the THEMIS data website http://themis.ssl.berkeley.edu. The geomagnetic *Kp* index was provided by the World Data Center C2 (WDC-C2) for Geomagnetism, Kyoto University (http://wdc.kugi.kyoto-u.ac.jp/index.html). This work was supported by BK21+ through the National Research Foundation (NRF) funded by the Ministry of Education of Korea. Work of K.-H. Kim was supported by the Basic Science Research Program through NRF funded by NRF-2013R1A1A2A10004414 and also supported by the project PE15090 of Korea Polar Research Institute.

The Editor thanks Jerry Goldstein and Dieter Bilitza for their assistance in evaluating this paper.

References

Angelopoulos, V. (2008), The THEMIS mission, *Space Sci. Rev.*, *141*, 5–37.
Bonnell, J. W., F. S. Mozer, G. T. Delory, A. J. Hull, R. E. Ergun, C. M. Cully, V. Angelopoulos, and P. R. Harvey (2008), The Electric Field Instrument (EFI) for THEMIS, *Space Sci. Rev.*, *141*, 303–341.
Carpenter, D. L. (1970), Whistler evidence of the dynamic behavior of the duskside bulge in the plasmasphere, *J. Geophys. Res.*, *75*, 3837–3847.
Carpenter, D. L., and R. R. Anderson (1992), An ISEE/whistler model of equatorial electron density in the magnetosphere, *J. Geophys. Res.*, *97*, 1097–1108.
Chappell, C. R., K. K. Harris, and G. W. Sharp (1970), A study of the influence of magnetic activity on the location of the plasmapause as measured by OGO 5, *J. Geophys. Res.*, *75*, 50–56.
Chappell, C. R., K. K. Harris, and G. W. Sharp (1971), The dayside of the plasmasphere, *J. Geophys. Res.*, *76*, 7632–7647.
Gallagher, D. L., P. D. Craven, and R. H. Comfort (2000), Global core plasma model, *J. Geophys. Res.*, *105*(A8), 18,819–18,833.
Gary, S. P., M. B. Moldwin, M. F. Thomsen, D. Winske, and D. J. McComas (1994), Hot proton anisotropies and cool proton temperatures in the outer magnetosphere, *J. Geophys. Res.*, *99*(A12), 23,603–23,615.
Goldstein, J., B. R. Sandel, M. F. Thomsen, M. Spasojević, and P. H. Reiff (2004), Simultaneous remote sensing and in situ observations of plasmaspheric drainage plumes, *J. Geophys. Res.*, *109*, A03202, doi:10.1029/2003JA010281.
Higel, B., and L. Wu (1984), Electron density and plasmapause characteristics at 6.6 R_E: A statistical study of the GEOS 2 relaxation sounder data, *J. Geophys. Res.*, *89*(A3), 1583–1601.
Hyun, K., K.-H. Kim, E. Lee, H.-J. Kwon, D.-H. Lee, and H. Jin (2014), Loss of geosynchronous relativistic electrons by EMIC wave scattering under quiet geomagnetic conditions, *J. Geophys. Res. Space Physics*, *119*, 8357–8371, doi:10.1002/2014JA020234.
Kim, K.-H., J. Goldstein, and D. Berube (2007), Plasmaspheric drainage plume observed by the Polar satellite in the prenoon sector and the IMAGE satellite during the magnetic storm of 11 April 2001, *J. Geophys. Res.*, *112*, A06237, doi:10.1029/2006JA012030.
Kwon, H.-J., et al. (2012), Local time-dependent Pi2 frequencies confirmed by simultaneous observations from THEMIS probes in the inner magnetosphere and at low-latitude ground stations, *J. Geophys. Res.*, *117*, A01206, doi:10.1029/2011JA016815.
Kwon, H.-J., K.-H. Kim, C.-W. Jun, K. Takahashi, D.-H. Lee, E. Lee, H. Jin, J. Seon, Y.-D. Park, and J. Hwang (2013), Low-latitude Pi2 pulsations during intervals of quiet geomagnetic conditions ($Kp \leq 1$), *J. Geophys. Res. Space Physics*, *118*, 6145–6153, doi:10.1002/jgra.50582.
Li, W., R. M. Thorne, J. Bortnik, Y. Nishimura, V. Angelopoulos, L. Chen, J. P. McFadden, and J. W. Bonnell (2010), Global distributions of suprathermal electrons observed on THEMIS and potential mechanisms for access into the plasmasphere, *J. Geophys. Res.*, *115*, A00J10, doi:10.1029/2010JA015687.
McFadden, J. P., C. W. Carlson, D. Larson, M. Ludlam, R. Abiad, B. Elliott, P. Turin, M. Marckwordt, and V. Angelopoulos (2008), The THEMIS ESA plasma instrument and in-flight calibration, *Space Sci. Rev.*, *141*, 277–302, doi:10.1007/s11214-008-9440-2.
Moldwin, M. B., M. F. Thomsen, S. J. Bame, D. J. McComas, and K. R. Moore (1994), An examination of the structure and dynamics of the outer plasmasphere using multiple geosynchronous satellites, *J. Geophys. Res.*, *99*, 11,475–11,481.
Moldwin, M. B., L. Downward, H. K. Rassoul, R. Amin, and R. R. Anderson (2002), A new model of the location of the plasmapause: CRRES results, *J. Geophys. Res.*, *107*(A11), 1339, doi:10.1029/2001JA009211.

Mozer, F. S. (1973), Analyses of techniques for measuring DC and AC electric fields in the magnetosphere, *Space Sci. Rev.*, *14*(2), 272–313, doi:10.1007/BF02432099.

Nishimura, Y., et al. (2013), Structures of dayside whistler-mode waves deduced from conjugate diffuse aurora, *J. Geophys. Res. Space Physics*, *118*, 664–673, doi:10.1029/2012JA018242.

Nishimura, Y., J. Bortnik, W. Li, L. R. Lyons, E. F. Donovan, V. Angelopoulos, and S. B. Mende (2014), Evolution of nightside subauroral proton aurora caused by transient plasma sheet flows, *J. Geophys. Res. Space Physics*, *119*, 5295–5304, doi:10.1002/2014JA020029.

O'Brien, T. P., and M. B. Moldwin (2003), Empirical plasmapause models from magnetic indices, *Geophys. Res. Lett.*, *30*(4), 1152, doi:10.1029/2002GL016007.

Pedersen, A., F. Mozer, and G. Gustafsson (1998), Electric field measurements in a tenuous plasma with spherical double probes, in *Measurement Techniques in Space Plasmas: Fields*, vol. 103, edited by R. F. Pfaff, J. E. Borovsky, and D. T. Young, pp. 1–12, Geophys. Monogr. Ser., AGU, Washington, D. C.

Summers, D., B. Ni, and N. P. Meredith (2007), Timescales for radiation belt electron acceleration and loss due to resonant wave-particle interactions: 1. Theory, *J. Geophys. Res.*, *112*, A04206, doi:10.1029/2006JA011801.

Takahashi, K., D.-H. Lee, M. Nose, R. R. Anderson, and W. J. Hughes (2003), CRRES electric field study of the radial mode structure of Pi2 pulsations, *J. Geophys. Res.*, *108*(A5), 1210, doi:10.1029/2002JA009761.

Takahashi, K., et al. (2010), Multipoint observation of fast mode waves trapped in the dayside plasmasphere, *J. Geophys. Res.*, *115*, A12247, doi:10.1029/2010JA015956.